Stability Enhancement of Perovskite Solar Cells Using Mixed Cation/HalidePerovskite

Ethan Eisenberg

George W. Hewlett High School

60 Everit Ave, Hewlett, NY 11557

Jack Cox

South Side High School

140 Shepherd St, Rockville Centre, NY 11570

Table of Contents

Section **Pages**

BACKGROUND

A lack of renewable resources requires exploring and utilizing alternative forms of energy e.g. solar energy (Fan, *et al.*, 2014**)**. There are various types of solar cells, including organic-inorganic photovoltaics, amorphous- silicon cells, dye-sensitized cells that involve the use of an organic dye, perovskites, and quantum dots that consist of nanoscale semi-conducting material (Fan *et al*., 2014). In recent years, organic-inorganic hybrid perovskite solar cells (PSCs) have emerged as a potential asset for thin film, low cost photovoltaics (H.J. Snaith, 2013). Perovskites have the common structure ABX_3 that is comprised of a monovalent cation, A=cesium (Cs+), methylammonium (MA), formamidinium (FA); (Saliba *et al.*, 2016), a divalent metal; B=(Pb^{2+}; Sn^{2+}) (Kim *et al.,* 2012; Stoumpos *et al,* 2014); and a halide anion X=(Cl^-, Br^-; I^-) (Noh *et al,* 2013). These materials have been shown to be beneficial in their optoelectronic capabilities. Perovskites exhibit high optical absorption coefficients (De Wolf *et al.* 2012) and long charge carrier diffusion lengths in the micrometer range (Xing *et al.*, 2013). Perovskite solar cells also have tunable bandgaps, ambipolar carrier transport, and a high resistance to impurities (Xiao, *et al.*, 2017). These properties have allowed their power conversion efficiency (PCE) to dramatically increase from 3.8% (Kojima *et al*., 2009) in 2009 to 22.1% (Green *et al.*, 2016; Yang *et al.*, 2017) in 2016, which exceeds the increase in efficiency for any other photovoltaic material **(**Correa-Baena *et al.,* 2017). Figure 1 depicts the evolution of perovskite cells in comparison to other thin film developments (Fan, *et al*., 2014). Furthermore, perovskites have shown to be beneficial by the ways in which they can be processed. For example, perovskites can be layered using one-step spin coating (Teuscher *et al.,* 2012), two-step sequential deposition (Xiao, *et al.,* 2017) , dip coating (Burschka *et al.*, 2017), 2step interdiffusion (Xiao *et al.,* 2014), or vacuum assisted evaporation (Li *et al.,* 2016). Most of these techniques involve a low temperature and are solution-based, and are therefore optimized for low cost commercialization.

The highest reported efficiencies have been attained with perovskites involving the implementation of methylammonium and formamidinium cations, and Bromine/Iodine halides

(Jeon *et al.*, 2015; Li *et al.* 2016). Recently, Cs was implemented to form mixed cation perovskite structures. Examples include: Cs/Ma, Cs/FA, or Cs/MA/FA compositions (Saliba *et al.*, 2016; Yi *et al.*, 2016; Li *et al.*, 2016) .

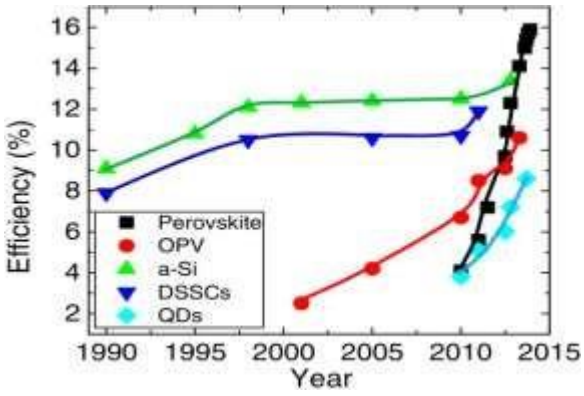

Figure 1: Evolution of Photovoltaic Thin Film Technologies (Fan, *et al.*, 2014)

Despite its advantages, perovskites are limited by their instability. Single organic cation perovskite cells such as $FAPbI_3$ or the $MAPbI_3$ classic structure degrade when left in ambience. Figure 2 shows three separate conditions by which perovskites were tested for their efficiency. Relative humidity is one factor that can affect its efficiency and stability (Han**,** *et al.*, 2015).

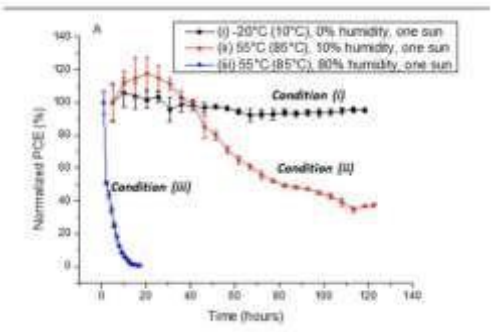

Figure 2: Stability Testing of Perovskite Solar Cells Under Three Different Environmental Conditions (Han, *et al.*, 2015)

Moreover, perovskites are also limited in their overall efficiency by their open-circuit voltage (Voc), which can be improved upon by filtering charge carriers through a photoactive layer (Seo *et al.*, 2016; Albrecht *et al.*, 2016; Hadadian *et al.*, 2016). The overall efficiency of perovskite cells are also limited by the crystal quality, in which impurities are found in FAbased

perovskites such as $FAPbI_3$ (Saliba *et al.*, 2016). In these PSCs, a yellow, photo-inactive polymorph phase exists, which includes a wider bandgap. This is referred to as the delta phase, and restricts electron movement.

Here we report the enhancement of perovskite solar cell efficiency and stability when exposed to 76% moisture. A one-step spin coating method was used to induce the perovskite thin film. The antisolvent chlorobenzene was added while spin coating to enable the formation of crystals. Moreover, a five-layered planar solar cell structure was used, as seen by Figure 3. Electrons were filtered through the perovskite photoactive layer to the TiO_2 layer, and positive holes were filtered through the active layer to the Spiro-OMeTAD layer.

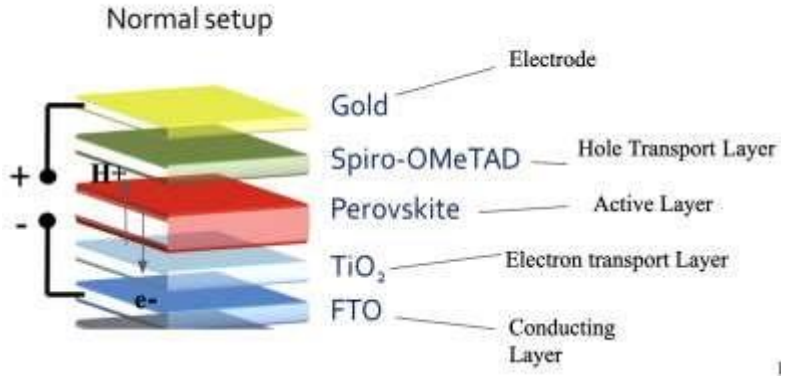

Figure 3: Layered Perovskite Structure (Physics Stack Exchange, 2017). This planar polycrystalline structure is an example of ambipolar carrier transport.

This study also investigates the use of a precursor solution to fabricate a CsFAMAPbIxBr1-x mixed cation/halide perovskite structure. Cs and formamidinium (FA) cations and a Br halide are believed to reduce the degradation of the perovskite cell in ambience. Moreover, FA is believed to provide a preferable band gap of approximately 1.4 eV, allowing for the greater excitation of electrons[Figure 4].

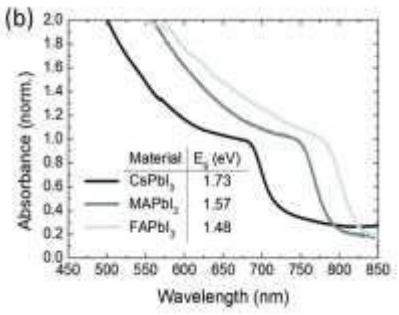

Figure 4: Relative UV- Absorption of Three Different Perovskite Materials (Xiao, *et al.*, 2017). $FAPbI_3$ has the smallest bandgap, and is associated with greater UV-absorbance and electric current output.

Through implementation of the mixed cation/halide structure and a post annealing temperature of 120 °C, we suppressed the delta-FAPbI3 perovskite. MA/FA/Pb/I/Br perovskite samples also exhibited higher open circuit voltages and short-circuit current densities when compared to classic MAPbI3 structure. A notable 14.03% efficiency was attained, an achievement when compared to the 12% efficient control perovskite. Consequently, surface morphology revealed an increase in grain size, proving the existence of a highly compact and relative smooth thin film, as well as a thin film with greater conductive material.

Research Problem/Hypothesis

Problem: How does a mixed cation/halide perovskite structure influence the stability and efficiency of perovskite solar cells?

Hypothesis: The mixed cation/halide structure will enhance both the stability and efficiency of the cell. The formamidinium cation is believed to optimize the bandgap, as seen when it is placed in the $FAPbI_3$ structure. This bandgap is 1.48 eV, which is preferable in that there is a lower distance required for the electrons to travel from the valence band to the conduction band, allowing for them to be more easily excited[Figure 4]. In addition, the Cs cation and Br halide are believed to enhance the stability of the perovskite cell by reducing degradation into its yellow photo inactive phase. By reducing phase transformation and optimizing the bandgap, the perovskite solar cell is believed to have enhanced absorption, efficiency, and stability.

Materials and Methods

The planar polycrystalline cell was prepared in 5 different layers: the FTO conductive layer, the TiO2 electron transport layer, the perovskite photoactive layer, the Spiro-OMeTAD hole transport layer, and gold electrodes. This design allowed for electrons and holes to be filtered through the perovskite active layer, with holes traveling to their respective location above the perovskite film, and the electrons filtering below the perovskite film.

Cleaning of the FTO Layer:

Fluorine-doped tin oxide(FTO) glass pieces (Sigma Aldrich) were initially cut into 1.4cm x 1.4cm wafers. They were then placed in 50 ml of acetone (99.9%) solvent. This was done under a fume hood. With distilled water serving as the medium, the wafers were sonicated for 10 minutes to vibrate the material and remove possible contaminants. To add on, the FTO slides bathed in isopropyl alcohol (99.5%) were sonicated for 10 minutes. The FTO slides were then bathed in ethyl alcohol (200 proof) while sonicated for 10 minutes. Next, a UV-Ozone facility emitted ionized oxide (O_3) in combination with UV-light to allow for a more cleaned surface. This was done for 15 minutes. After cleaning, FTO wafers were tested for their ohmic value using a multimeter to determine electric resistance, and therefore, which side of the FTO glass was conductive. If the multimeter revealed values of 1 or infinity, then that given side was not conductive.

Preparation of the TiO_2 Electron Transport Layer

TiO_2 precursor was prepared through the following process:

First, 1 milliliter of Titanium (IV) butoxide with 97% purity was dissolved in 10 milliliters of ethanol for 30 minutes. 1 mL of ethanoic acid (99%) was then added and stirred for 30 minutes using a magnetic stirrer (stir bar). Next, 1 mL of acetylacetone(99%) was added and stirred for 30 minutes. 1 milliliter of deionized water was then added and stirred for 30 minutes.

After the precursor was prepared, FTO pieces were spin-coated with the TiO_2 solution at 2,000 rpm for 30 seconds to produce a thin film. This was completed under a fume hood. Once spin casted, the washed FTO glasses were pyrolyzed on a hotplate at 465 °C for two hours, inducing the formation of an electron transport layer (ETL) through a sol-gel (chemical solution deposition) reaction. This was also completed under the fume hood.

To observe morphological data by scanning electron microscopy and atomic force microscopy, glass pieces were required to be cut using diamond cutters into 1.3cm by 1.3 cm wafers. The washing and spin casting process was identical to the FTO glass.

Addition of the Perovskite Precursor, Spiro-OMeTAD, and Gold Electrodes

The one-step spin-coating method was used to prepare the mixed cation/halide perovskite film:

First, PbI_2, MAI, CsI, FAI, and $PbBr_2$ at a molar ratio of 1:.7:0.15:0.15 were placed in a mixed solvent of Dimethyl Formamide (DMF) and Dimethyl Sulfoxide (DMSO) (8:2) and left overnight in a magnetic stirrer. The molar ratio allowed for a distribution of the mixed cation/halide components into three categories: the main, minor, and additive. FAI and PbI-----$_2$ comprised of 85%, and served as the main of the perovskite, MABr, and $PbBr_2$ comprised of 10% and served as the minor of the perovskite, and CsI comprised of only 5%, acting as the additive. The perovskite was uniformly mixed. The perovskite precursor was deposited onto the TiO_2 -glass via spin coating at 4,000 rpm for 30 seconds. Acting as the antisolvent, chlorobenzene (99.9%) was then dipped onto the surface to induce crystal generation. Next, the as casted film was annealed at 100 °C for 10 minutes. The Spiro-OMeTAD layer was then coated using spin casting at 4,000 rpm for 30 seconds to induce a hole-transport layer (HTL). Lastly, physical vapor deposition (PVD) was used to add the gold electrodes. The perovskite

(photoactive layer) and Spiro-OMeTAD(HTL) were added in a glove box where temperature and humidity were regulated to prevent facile degradation.

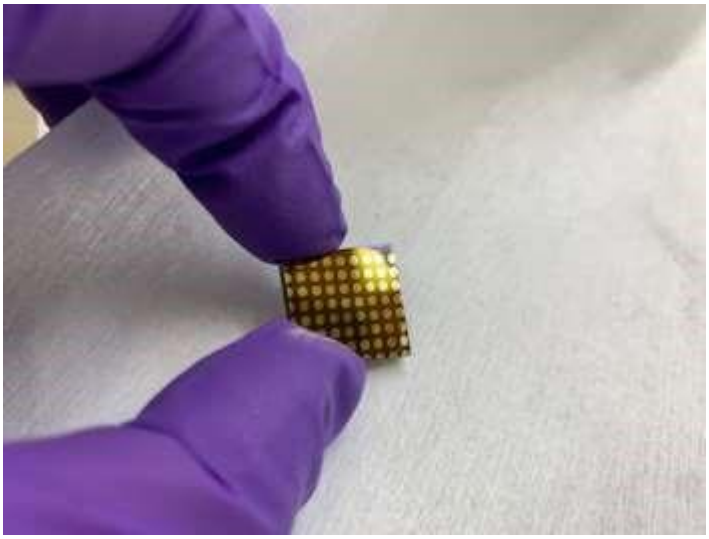

Completed Perovskite Device

RESULTS and DISCUSSION

To investigate the surface morphology of the mixed cation/halide perovskite, scanning electron microscopy (SEM) was performed. Two magnifications (20.0k and 50.0k) were obtained for both the $MAPbI_3$ (Control) Perovskite and CsFAMAPbIxBr1-x (Mixed) Perovskite. An increase in crystal size would indicate the presence of more conductive material for light absorption, and thus the possibility for a greater power conversion efficiency. As seen in Figure 5, the mixed perovskite had a highly crystalline surface. SEM revealed the presence of non-conductive areas between crystal grains known as grain boundaries. These grain boundaries deteriorate optoelectronic performance by restricting the movement of electrons and holes. With the increased grain size of the mixed perovskite, the grain boundaries were reduced, supporting the notion that the mixed perovskite provided more conductive material for UV-light absorption.

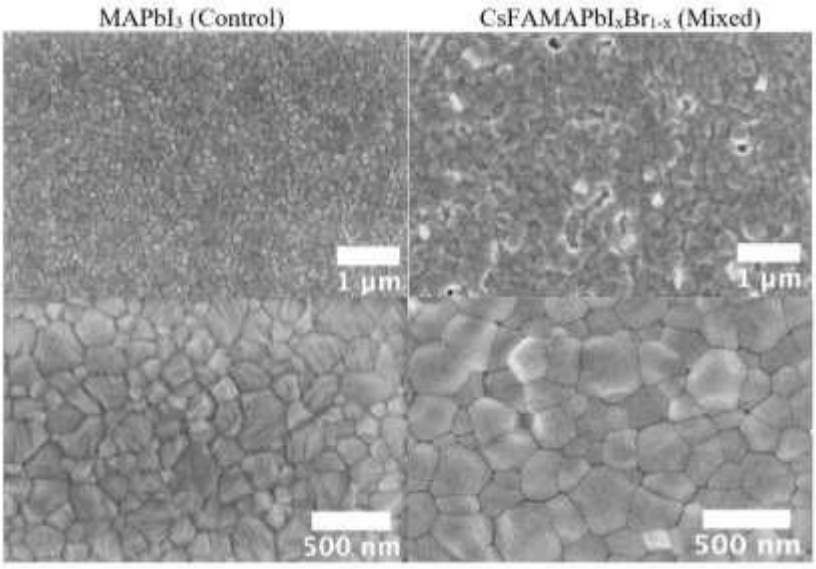

Figure 5: SEM Images of the MAPbI3Control Perovskite and the CsFAMAPbIxBr1-x(Mixed) Perovskite 3.0kV 5.6mm x 20.0k SE(U) and 3.0kV 5.6mm x 50.0k SE(U) .

To determine the average gain size, an imaging analysis tool known as "Nanoscale Measurer" was used. As seen in Figure 6, the control MAPbI3 perovskite exhibited an average grain size of 194 nm, and the CsFAMAPbIxBr1-x perovskite showed a greater average grain size of 268 nm.

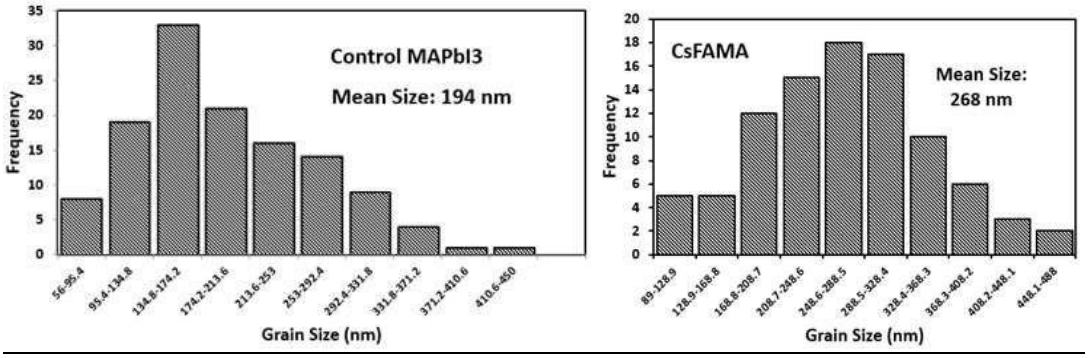

Figure 6: Crystal Grain Size Distribution for the Control MAPbI3 Perovskite and the CsFAMAPbIxBr1x(Mixed) Perovskite

To investigate the surface topography and roughness of the mixed cation/halide perovskite cell, contact atomic force microscopy was performed. Two readings of the surface were obtained for both the $MAPbI_3$ (Control) Perovskite and CsFAMAPbIxBr1-x (Mixed) Perovskite. If there is a large increase in roughness, the cell's ability to absorb light will be compromised. As seen in Figure 3, the cell's roughness (RMS) varied from 10.5 nm for the control to 20.4 nm for the mixed cation/halide structure. Despite this change, the roughness varied within an acceptable range, proving the formation of a relatively smooth polycrystalline film. The AFM results were also correspondent to that of the SEM with an increase in grain size.

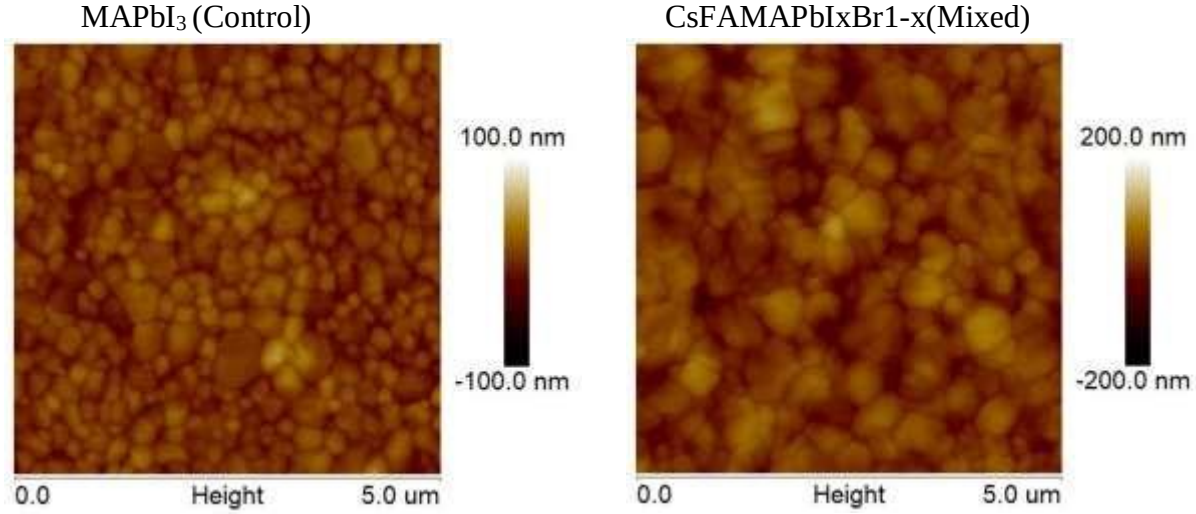

Figure 7: AFM images of the $MAPbI_3$Control Perovskite and the CsFAMAPbIxBr1-x(Mixed) Perovskite. The AFM revealed the presence of a relatively smooth surface, allowing for a high absorption coefficient.

To determine if the perovskite contains a cubic or hexagonal structure, or the type of crystal phase present, X-Ray Diffraction was performed. There are two possible phases that could exist within the perovskite cell: a delta phase or an alpha phase. If it was observed that there was a delta phase present, the cell was not optimized for its optoelectronic capabilities. A

delta phase is hexagonal and is photo inactive, meaning it is unable to absorb light. Conversely, an alpha phase is cubic and photo active, meaning it is able to absorb light. To determine the crystal shapes present, a set of three numbers known as a Miller Index was utilized. Figure 8 represents the X-Ray Diffraction Spectra of CsFAMA, FAMA, and KCsFAMA perovskite films.

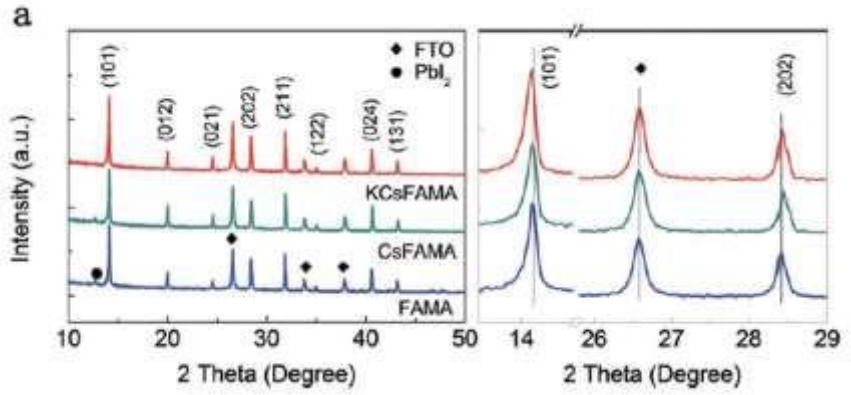

Figure 8: XRD patterns of FAMA/CsFAMA/KCsFAMA perovskite films(Bu *et al.*). These patterns were utilized to identify the major peaks of the mixed cation/halide perovskite film with their respective Miller indices(Bu *et al.*, 2017).

Results implicated that both alpha and delta phases were present within the mixed cell, with only the alpha phase being active. In contrast, the control $MAPbI_3$ perovskite had a single peak with a Miller index of 100, indicating that it is cubic and photoactive. Therefore, the mixed perovskite layer was annealed at various conditions to reduce the hexagonal delta phase and enhance the alpha photoactive phase. Through changing the post- annealing temperature from 100 °C to 120 °C, there was a preferable crystallization of the mixed perovskite with a strong alpha peak and negligible delta phase[Figure 9]. In turn, the changing of the post annealing temperature reduced the presence of the photo inactive phase within the cell.

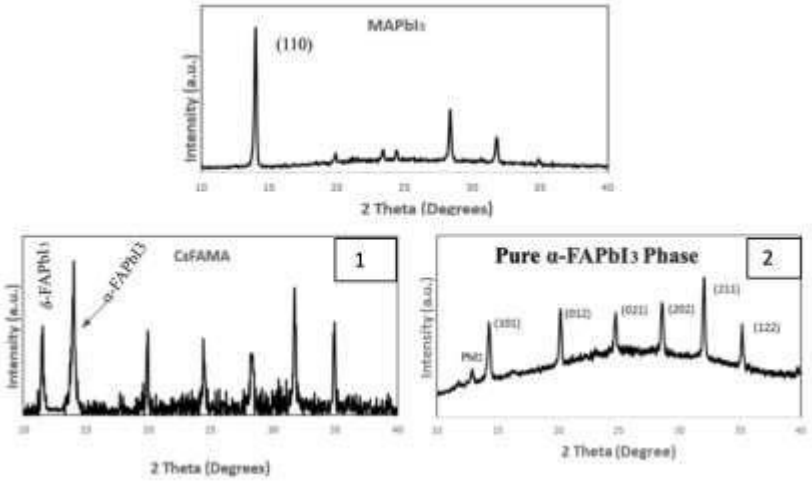

Figures 9,9-1,9-2: XRD Images of the $MAPbI_3$Control Perovskite and the CsFAMAPbIxBr1-x(Mixed) Perovskite Figure , CsFAMAPbIxBr1-x(Mixed) Perovskite when annealed at 100 °C, CsFAMAPbIxBr1x(Mixed) Perovskite when annealed at 120 °C

To observe the UV-light absorption of the mixed perovskite, UV-Visible Spectroscopy was performed. If the perovskite's absorbance would decrease, less light would be absorbed, and therefore less electrons will reach their excited state necessary for the generation of a current. It was observed that the absorbance showed comparable spectral patterns to that of the control, indicating that the implementation of the mixed cation/halide structure did not compromise the light absorbing ability of the perovskite.

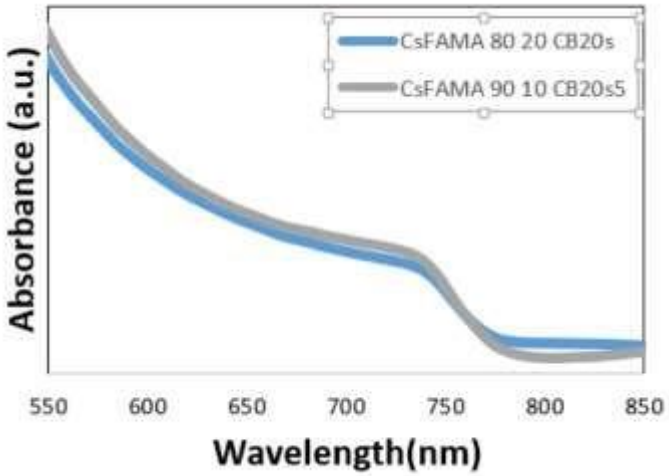

Figure 10: UV-Visible Spectrum for the CsFAMAPbIxBr1-x(Mixed) Perovskite

To investigate the efficiency of the mixed perovskite cell, the device was connected to an electrode. Voltages and current densities were measured, with the short-circuit current density (Jsc) existing when the voltage is 0, and the open-circuit voltage (Voc) existing when the current density is 0. The values of the current density and voltage were used to generate the J-V curve. The J-V curve was then used to determine efficiency as seen by formula: Power Conversion Efficiency (PCE) =Jsc x Voc x Fill Factor(FF). The Fill factor was determined by calculating the area under the curves at each of their respective turning points, as seen in figure 6. The power conversion efficiency can also be calculated using the formula PCE= Maximum current density(Jm) x Maximum Voltage (Vm). Results revealed that the power conversion efficiency of the photovoltaic increased from 12.20% for the non-mixed perovskite to 14.03% for the CsFAMAPbIxBr1-x (Mixed) perovskite[Table 1].

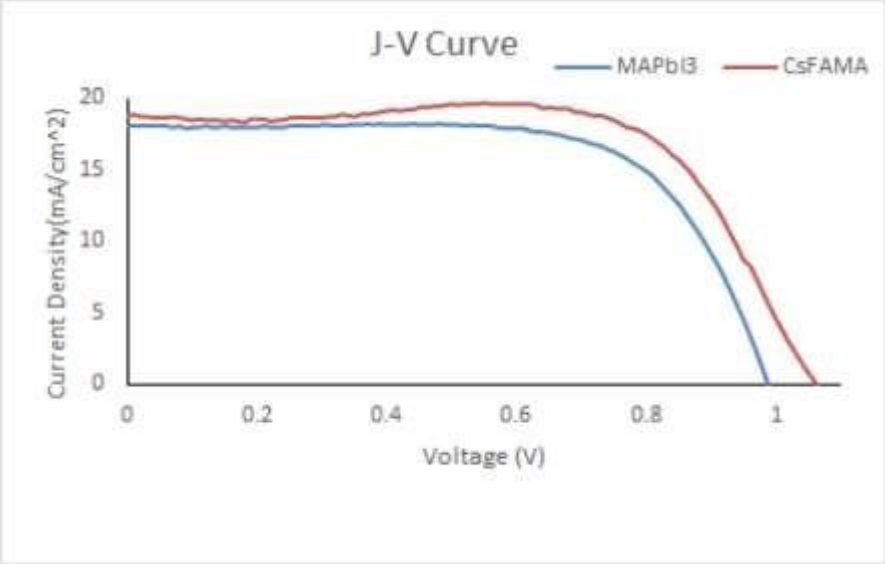

Figure 11: J-V efficiency curves for both the MAPbI$_3$Control Perovskite and the CsFAMAPbIxBr1-x(Mixed) Perovskite

	Jsc (mA/cm^2)	Voc (V)	FF	PCE (%)
Non-Mixed	18.09	0.985	0.68	12.20
CsFAMA	18.82	1.065	0.70	14.03

Table 1: Short-Circuit Current Densities(Jsc), Open-Circuit Voltages(V), Fill Factors, and Power-Conversion Efficiencies(%) for both the the MAPbI$_3$Control Perovskite and the CsFAMAPbIxBr1-x(Mixed) Perovskite

To investigate stability, X-Ray Diffraction was conducted in ambient conditions. A FAMA perovskite structure was compared to a completely mixed perovskite. The perovskite cells were tested for both the mixed and unmixed for 24 hours under 76% relative humidity to simulate environmental conditions. As seen in Figure 12, results revealed that the delta photo inactive phase and PbI2 impurities were greatly reduced with the addition of Cs, therefore enhancing the stability under intense heat, light, and moisture.

Therefore, results revealed that a perovskite with the mixed cation/halide structure CsFAMAPbIxBr1-x was successfully prepared using a solution-based spin casting method. The stability and surface morphologies of the cell were investigated to determine how these factors can be used to enhance device output. The morphology data implicated a fully covered, highly crystalline, and relatively smooth CsFAMA perovskite thin film. Moreover, the grain size increased with the CsFAMA perovskite, as compared to the non-mixed classical $MAPbI_3$ structure. X-Ray diffraction results revealed the existence of two crystal phases of $FAPbI_3$, an alpha photoactive phase and a delta photo inactive phase. To alleviate the presence of the delta phase and to optimize the optoelectronic properties of the cell, the post annealing temperature was changed from 100 ℃ to 120 ℃. By changing the temperature, there was a reduction in the non light-absorbing material. Moreover, there was an increase in power conversion efficiency, as shown by the J-V curves. Lastly, moisture and heat stability tests revealed the importance of Cs in preventing degradation. Other research studies have explored the prospect of a mixed cation/halide perovskite, but with different components and methods of preparation. One example is with the research team of Pellet el al., who investigated the MAxFA1-xPbI3 structure. The thin film was prepared through a sequential method, in which the mixed structure was fabricated through a reaction of pre-deposited PbI_2 films with methylammonium iodide (MAI) and formamidinium iodide (FAI) in isopropanol. Results revealed a correspondent bandgap to the $FAPbI_3$ structure. They also showed comparable results to the CsFAMA mixed structure in regard to the delta phase reduction, despite using a different method of thin film preparation (Xiao, Jia-Wen, *et al.*, 2017).

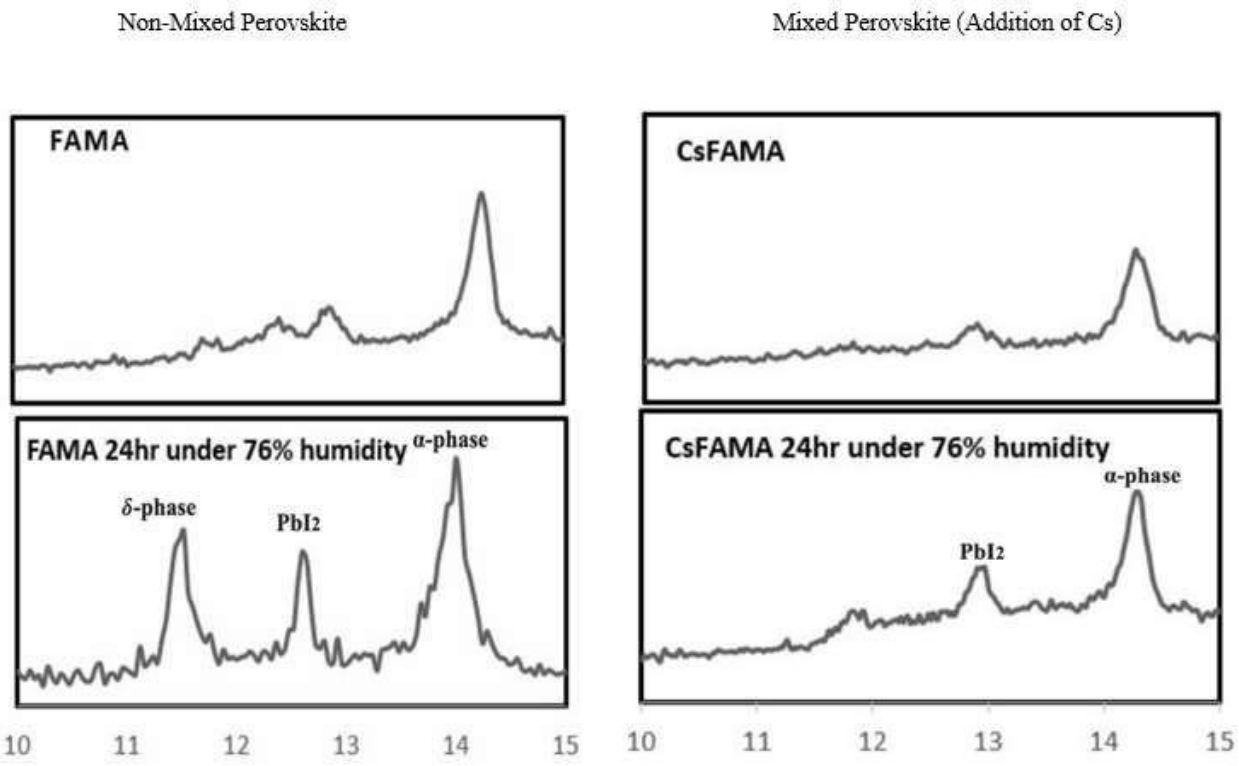

Figure 12: Stability tests for mixed and non-mixed perovskites when left in ambience for one full day

CONCLUSION

The hypothesis was supported by the results. It was shown that the implementation of the CsFAMAPbIxBr1-x mixed cation/halide perovskite structure increased the power conversion efficiency of the perovskite from 12.20% to 14.03%. Although visible spectroscopy revealed comparable shapes to the control, the mixed structure did not degreate the photovoltaic's light absorbing capabilities. Consequently, it was supported that there was the fabrication of a pure $FAPbI_3$ perovskite, eliminating the presence of the delta photo inactive phase.

FUTURE STUDIES

Although there was a notable success in stability and efficiency, our investigation of the mixed cation/halide perovskite has been limited by several factors. The first being that of statistical significance. Because perovskites easily degrade when exposed to intense heat, moisture, and

light, we were only able to test the efficiency of the perovskite once. In the future, we plan to engage in multiple trials for efficiency and determine the p-value using these measurements. This experiment was also constrained to a 5-week time interval, further hindering the potential for multiple trials. Despite these limitations, it is important to note that the efficiency measurement was correspondent to that of the surface morphology results, indicating its viability. Furthermore, different methods of thin-film fabrication can be used. Two-step spin coating, for example, is an alternate method for efficient and cheap perovskite formation(Bi *et al.*, 2013). Lastly, different concentrations of the cations and halides can be implemented into the mixed composition to enhance UV-absorption. Although FAI served as the main (85%) of the perovskite, the photovoltaic exhibited a comparable UV-Spectra to that of the control.

REFERENCES

A. Kojima, K. Teshima, Y. Shirai, T. Miyasaka, Organometal halide perovskites as visible light sensitizers for photovoltaic cells. J Am Chem Soc 131, 6050-6051 (2009).

B. R. Li et al., Chlorobenzene vapor assistant annealing method for fabricating high quality perovskite films. Org Electron 34, 97-103 (2016).

C. Y. Yi et al., Entropic stabilization of mixed A-cation ABX(3) metal halide perovskites for high performance perovskite solar cells. Energ Environ Sci 9, 656-662 (2016).

Correa-Baena, Juan-Pablo, et al. "The Rapid Evolution of Highly Efficient Perovskite Solar Cells." Energy & Environmental Science, vol.10,no. 3, 2017,., doi:10.1039/c6ee03397k.

D. Bi et al., Using a Two-Step Deposition Technique To Prepare Perovskite(CH3NH3PbI3) for Thin Film Solar Cells Based on ZrO2 and TiO2 Mesostructures.

F. Hao, C. C. Stoumpos, D. H. Cao, R. P. H. Chang, M. G. Kanatzidis, Lead-free solid-state organic-inorganic halide perovskite solar cells. Nature Photonics 8, 489-494 (2014).

Fan, Jiandong, et al. "Perovskite-Based Low-Cost and High-Efficiency Hybrid Halide Solar Cells." *Photonics Research*, Optical Society of America, 11 Aug. 2014, www.osapublishing.org/prj/abstract.cfm?URI=prj-2-5-111.

G. Xing et al., Long-range balanced electron- and hole-transport lengths in organic inorganic CH3NH3PbI3. Science 342, 344-347 (2013).

H. J. Snaith, Perovskites: The Emergence of a New Era for Low-Cost, High-Efficiency Solar Cells. J Phys Chem Lett 4, 3623-3630 (2013).

H. S. Kim et al., Lead iodide perovskite sensitized all-solid-state submicron thin film mesoscopic solar cell with efficiency exceeding 9%. Sci Rep 2, 591 (2012).

Han, Yu, et al. "Degradation Observations of Encapsulated Planar CH3NH3PbI3 Perovskite Solar Cells at High Temperatures and Humidity." *Journal of Materials Chemistry A*, The Royal Society of Chemistry, 9 Mar. 2015, pubs.rsc.org/en/content/articlelanding/2015/ta/c5ta00358j#!divAbstract.

J. Burschka et al., Sequential deposition as a route to high-performance perovskite sensitized solar cells. Nature 499, 316-319 (2013).

J. H. Noh, S. H. Im, J. H. Heo, T. N. Mandal, S. I. Seok, Chemical management for colorful, efficient, and stable inorganic-organic hybrid nanostructured solar cells. Nano Lett 13, 17641769 (2013).

J.-P. Correa-Baena et al., The rapid evolution of highly efficient perovskite solar cells. Energ Environ Sci 10, 710-727 (2017)

J. Y. Seo et al., Ionic Liquid Control Crystal Growth to Enhance Planar Perovskite Solar Cells Efficiency. Adv Energy Mater 6, 1600767 (2016).

M. A. Green et al., Solar cell efficiency tables (version 49). Progress in Photovoltaics: Research and Applications 25, 3-13 (2017).

M. Hadadian et al., Enhancing Efficiency of Perovskite Solar Cells via N-doped Graphene: Crystal Modification and Surface Passivation. Advanced materials 28, 8681-8686 (2016).

M. M. Lee, J. Teuscher, T. Miyasaka, T. N. Murakami, H. J. Snaith, Efficient hybrid solar cells based on meso-superstructured organometal halide perovskites. Science 338, 643-647 (2012).

M. Saliba et al., Cesium-containing triple cation perovskite solar cells: improved stability, reproducibility and high efficiency. Energy Environ Sci 9, 1989-1997 (2016).

N. J. Jeon et al., Compositional engineering of perovskite materials for high-performance solar cells. Nature 517, 476-480 (2015).

N. Pellet et al., Mixed-organic-cation perovskite photovoltaics for enhanced solar-light harvesting. Angew Chem Int Ed Engl 53, 3151-3157 (2014).

"Perovskite Solar Cells: Why Are Electron/Hole-Transporting Layers Required?" *Physics Stack Exchange*, Oct. 2017, physics.stackexchange.com/questions/363966/perovskite-solar-cells-whyare-electron-hole-transporting-layers-required.

S. Albrecht et al., Monolithic perovskite/silicon-heterojunction tandem solar cells processed at low temperature. Energy Environ Sci, (2016).

S. De Wolf et al., Organometallic Halide Perovskites: Sharp Optical Absorption Edge and Its Relation to Photovoltaic Performance. J Phys Chem Lett 5, 1035-1039 (2014).

T. Bu et al., A Novel Quadruple-Cation Absorber for Universal Hysteresis Elimination for High Efficiency and Stable Perovskite Solar Cells. Energy and Environmental Science (2017).

W. S. Yang et al., Iodide management in formamidinium-lead-halide–based perovskite layers for efficient solar cells. Science 356, 1376-1379 (2017).

Xiao, Jia-Wen, et al. "The Emergence of Mixed Perovskites and Their Applications as Solar

Cells.” Advanced Energy Materials, DOI:10.1002/aenm.201700491.3. Accessed 22 July 2019

X. Li et al., A vacuum flash-assisted solution process for high-efficiency large-area perovskite solar cells. Science 353, 58-62 (2016).

Zhou, Yuanyuan, and Yixin Zhao. “Chemical Stability and Instability of Inorganic Halide Perovskites.” Energy &1Environmental Science, vol. 12, no. 5, 2019,., doi:10.1039/c8ee03559h.

Acknowledgements:

We would like to thank Dr. Rafailovich for guiding the research endeavor.